Available online at **www.joac.info**

ISSN: 2278-1862

Journal of Applicable Chemistry

2019, 8 (6): 2423-2433

(International Peer Reviewed Journal)

Preparation of γ-Al_2O_3 from Industrial Waste Can and its use for the Adsorption of Metals: Cd(II) and Pb(II)

Najdat R. Al-Khafaji

Department of Chemistry, College of Science, University of Kufa, **IRAQ**

Email: najdat.alkhafaji@uokufa.edu.iq

Accepted on 5th November, 2019

ABSTRACT

Aluminium oxide is an important chemical due to its many valuable properties such as hard ware resistance, good thermal conductivity, high strength and stiffness. Aluminium oxide is commonly referred to as alumina. In the present study, several types of alumina were synthesized from sodium aluminate ($NaAlO_2$) by precipitation with sulfuric acid (H_2SO_4) and subsequently calcinations at 500°C to obtain γ-Al_2O_3. The various γ-Al_2O_3synthesized were characterized by X-ray diffraction (XRD), adsorption –desorption of N_2 (S_{BET}). XRD revealed that distinct phases of Al_2O_3 were formed during thermal treatment. Moreover, it was observed that conditions of synthesis (pH, aging time and temperature) strongly affect the physicochemical properties of the alumina. A high surface area alumina (370 $m^2 g^{-1}$) was synthesized under mild conditions, from inexpensive raw materials. These alumin as were tested for the adsorption of Cd (II) and Pb (II) from aqueous solution at toxic metal concentrations, and isotherms were determined

Graphical Abstract

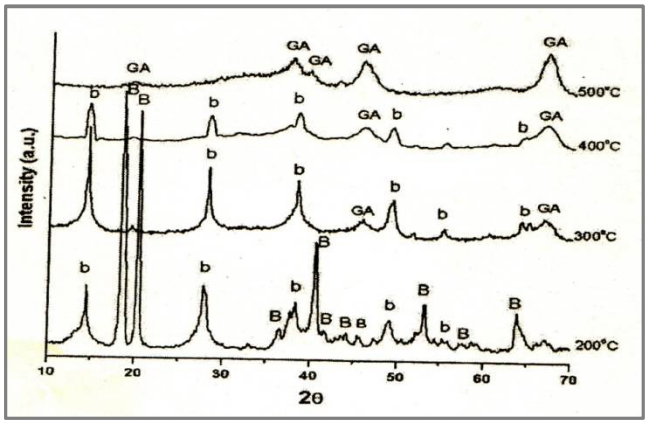

XRD patterns showing phases of alumina formed during calcination of (G7-75) (B:bayerite; b;boehmite; G:gibbsite ; GA :γ- Al_2O_3).

Keywords: X-ray diffraction, Aluminum oxides, Mesoporosity, Adsorption.

INTRODUCTION

Alumina has an important industrial application due to the pronounced physical and chemical properties [**1, 2**]. Refineries are familiar with the gamma phase due to its important use as catalyst support in the hydrotreating processes because of its large surface area, highly porous and excellent mechanical strength [**3**]. It is also used as a good adsorbent in many processes of drying, sweetening and filtration operations having high industrial potential [**4**]. Material with these characteristics have predominate industrial focus offering a long life when used as catalysts and adsorbents [**5**].

Aluminum oxide exists in many forms which are produced through the calcination of aluminum hydrates bayerite, gibbsite and boehmite at temperatures ranging between 230-1100°C [**6**]. In this thermal treatment, dehydration causes a series of decomposition and transformation producing different types of aluminum oxides starting from $Al(OH)_3$, to α-Al_2O_3 [**7**]. γ- Al_2O_3very important among other phases because of its structure possesses high surface which gains the focus for many chemical and petrochemical separation processes and catalysis [**8**]. Also it is used as a ceramic raw material and as gas sensor [**9**].

The use of adsorbents to treat wastewater has become an important topic of research, since adsorption processes are very simple, compared to chemical processes such as precipitation or ion-exchange. Additionally, in response to environmental quality requirements for drinking water, recent work includes the synthesis of new economical adsorbents with useful properties for contaminant removal, to replace conventional high-cost adsorbents (activated carbon, zeolites, SBA-15, etc.) [**10**].

Investigation for the synthesis of materials by the recycling of wastes are having the interest of many researchers because it solves important environmental problems , cost effective from an economics point of view ,in addition to its utilization in many potential applications . The aforementioned descriptions reflect the necessary aspects of green technologies [**11**].

A great amount of aluminum scrap is produced worldwide, of which a major part is recovered by recycling [**12**], but an alternative way of using the aluminum scrap is to transform it directly into alumina, which finds several uses (in catalysts, in soft abrasives, in coatings and in adsorbents). The aim of this study was to synthesize alumina by acidic precipitation of sodium aluminate.

MATERIALS AND METHODS

Preparation of γ- alumina: Scrap metal aluminum from beverage cans (99.9% pure) reacted, at room temperature, with a stoichiometric amount of 2N aqueous NaOH in a batch reactor to produce a solution of sodium aluminate ($NaAlO_2$). This solution was passed through filter paper and the clear filtrate was neutralized with 2N H_2SO_4, to pH 6, 7 or 8, resulting in the precipitation of a white gel, $Al(OH)_3 \cdot XH_2O$. Some aliquots of the synthesized gel were left to stand for 48 h (aging time) in the mother liquor at room temperature (approximately 25 °C), while others were left for a period of 4 h at 75°C. The resulting gel samples were named as G 6-25, G 7-25, G 6-75, G 7-75 and G 8-75, according to the pH at which each gel was precipitated and the aging temperature; for example, G 6-25 was obtained at pH 6 and aged at 25°C, while G 7-75 was obtained at pH 7 and aged at 75°C. Following the aging step, the gels were washed until no more sulfate ions were detected in the washings. Finally, they were dried at 75°C for 6 h, then ground and passed through a 60 mesh sieve. The samples were then calcined for 3 h in a muffle furnace, in air, at a heating rate of 5°C min^{-1}. Analogously to the gel samples, calcined samples were named: Al -Ox 6-25, Al -Ox7-25, Al -Ox6-75, Al -Ox7-75 and Al -Ox 8-75.

Characterization: The crystalline phases present in the aluminum hydroxides and calcined oxides were identified by X-ray diffraction (XRD), using Cu-K radiation (λ=1.5404) generated at 40 kV and 30 mA, in which the Bragg angle (2θ) was scanned between 4° and 70 °.

The porous structure of the aluminas was characterized by adsorption–desorption of N_2 (BET method) at the temperature of liquid nitrogen (77 K), with a Micromeritics instrument. The gas used for analysis was 99.9% pure. The dry materials were previously degassed at 200°C, in order to remove water and any impurities physisorbed on the solid surface.

Adsorption essay: Stock solutions of 1000 mg L^{-1} Cd(II), and lead Pb(II) in distilled water were prepared from the salt precursors $Cd(NO_3)_2{\cdot}4H_2O$ and $Pb(NO_3)_2{\cdot}4H_2O$ (Merck) respectively. By diluting these stock solutions, the working solutions for adsorption tests were prepared.

The adsorption isotherms were performed under favorable conditions for the adsorption of cadmium and lead, respectively, as previously determined: contact time (adsorbent/adsorbate) of 7 h, magnetic stirring at 400 rpm, adsorbent load in solution (w/v) = 8 g L^{-1}, initial pH of cadmium solutions = 5, pH of lead solution =3 and all solutions at room temperature (approximately 25°C). The concentration of metal ion varied from 10 to 200 mg L^{-1}. The initial pH of the metal solutions was adjusted by adding 0.1 M HNO_3 or 0.1 M NaOH.

After reaching equilibrium, the mixture (adsorbate/adsorbent) was filtered through a cellulose membrane (Millipore, 0.45 μm). The contents of Cd(II) and Pb(II) in the filtrates were analyzed in an Atomic Absorption Spectrophotometer (Perkin Elmer 3100) provided with hollow cathode lamps for cadmium (λ = 228.8 nm) and lead (λ = 217.0 nm).

In the field of adsorption of contaminants, the parameter qe (mg of adsorbate g^{-1} of adsorbent), which measures the adsorptive capacity of the adsorbent, and the adsorption isotherms are both widely used to characterize the adsorption process. The adsorption capacity of alumina was calculated as follows:

$q_e = V{\cdot}(C_i - C_e)/m$, where C_i is the initial concentration of the metal in solution (in mg L^{-1}) and C_e its concentration at equilibrium, V is the volume of solution in liters, m is the weight of the adsorbent (alumina) in grams and q_e is the adsorption capacity (mg g^{-1}) at equilibrium. In liquid–solid systems, the isotherm models most used are:

Freundlich isotherm: Based on the assumption that the adsorbing surface is energetically heterogeneous, consisting of adsorption sites of differing energies. The linearized form of the Freundlich equation is as follows:

$$\log q_e = \log K_f + \frac{1}{n} \log C_e \qquad (1)$$

Where q_e is the amount of adsorbate retained per gram of adsorbent (mg g^{-1}), C_e is the concentration of adsorbate (mg L^{-1}) at equilibrium, and K_f and n are Freundlich constants related to the adsorption capacity and adsorption intensity, respectively**.**

Langmuir isotherm: Based on the assumption that all adsorption active sites are equivalent and that the ability of a molecule to interact with a site on the surface of the adsorbent is independent of whether neighboring sites are occupied or not. In addition, adsorption is restricted to a monolayer and there are no lateral interactions between adsorbed molecules. The linearized form of this isotherm is represented by the following equation:

$$\frac{C_e}{q_e} - \frac{1}{q_{max}\, b} + \frac{C_e}{q_{max}} \qquad (2)$$

Where C_e and qe are as defined previously (mg g^{-1} adsorbent), q_{max} (mg g^{-1}) and b (L mg^{-1}) are Langmuir constants related to the maximum adsorption capacity and adsorption energy, respectively.

RESULTS AND DISCUSSION

The crystalline nature of the synthesized gels was analyzed by X-ray diffraction (XRD), the resulting patterns being shown in (figures 1 and 2). The patterns show peaks of peaks related to the crystal phases of bayerite, boehmite and gibbsite.

It can be seen from these results that precipitation at acidic or neutral pH (pH 6-7) did not modify the crystal structure significantly ,since the XRD patterns of the four samples : G 6-25, G 7-25, G 6-75 and G 7-75 and are similar and contain a principal phase of bayerite and a minor phase of boehmite. On the other hand, precipitation at basic pH 8, led to the formation of mainly gibbsite phase and bayerite in lower proportion.

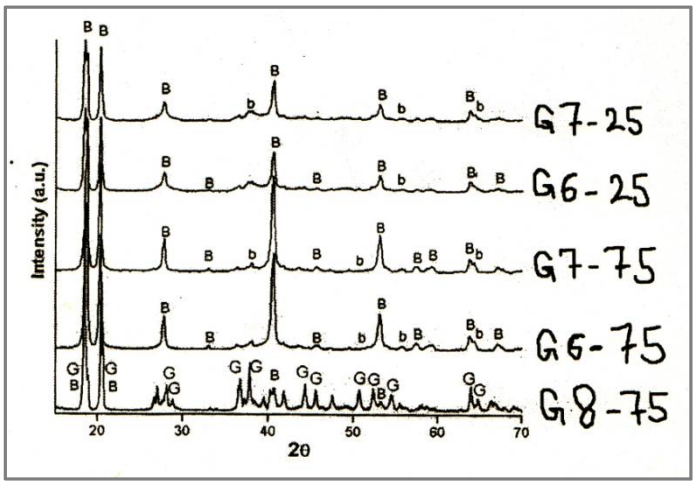

Figure 1. XRD patterns of aluminum hydroxides synthesized under various conditions of aging temperature and pH of precipitation (B: bayerite; b;boehmite; G:gibbsite) .

The XRD patterns in (figure 2) show that the samples precipitated at pH 7 and aged at room temperature for 2 h (G 7-25 2h) and 48 h (G 7-25 2h) and one sample aged for 4h at 75°C (G 7-75). These results indicate that the aged for only 2h is amorphous, meaning that 2h of aging at 25°C is not sufficient to form crystals of boehmite and bayerite. These crystals are only formed over long aging times (48h) at room temperature, or short aging times at 75°C.

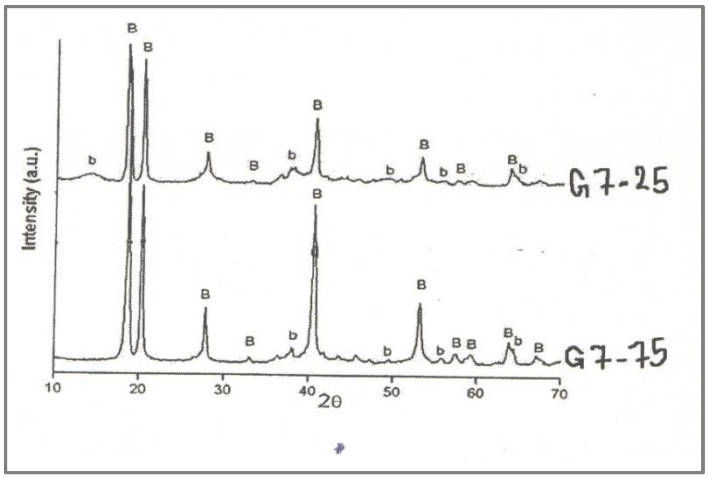

Figure 2. XRD patterns of aluminum hydroxides aged under various conditions (B:bayerite; b;boehmite; G:gibbsite).

The degree of crystalline apparent in the diffraction patterns of G 7-75 and G 7-75 (figure 1) indicates that there is an inverse relationship between aging temperature and aging time, High temperature accelerates the formation of large crystals : thus at high temperature fewer grains are formed, allowing an orderly growth (nucleation process). According to Rinaldi [**13**], during aging, particles of aluminium hydroxide are solubilized and growth takes place through condensation reactions: this growing process can be accelerated at high temperatures, leading to the formation of particles of large size.

The phases formed during the calcination of (G 7-75) at temperature of 200, 300, 400 and 500°C, are shown in (figure 3) In this figure , the sample calcined at 200°C, the most intense peak correspond to the bayerite phase, but peaks of relatively low intensity indicating boehmite are also seen. An unexpected increase in the intensity of both bayerite and boehmite peaks. At 300°C, the peaks for bayerite disappeared and the majority phase was highly crystalline boehmite, while small peaks attributed to gamma alumina (γ-Al_2O_3) were formed.

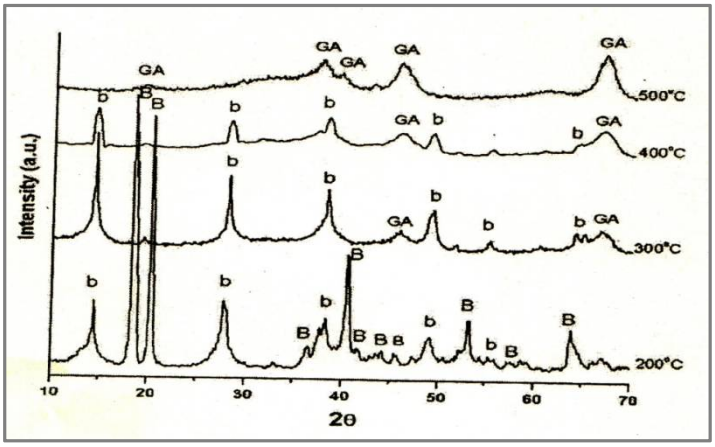

Figure 3. XRD patterns showing phases of alumina formed during calcination of(G7-75) (B:bayerite; b;boehmite; G:gibbsite ; GA :γ- Al_2O_3).

The boehmite formed at 300°C lost some crystallinity and the gamma alumina peaks became more noticeable. At 500°C, a single phase of gamma alumina (γ- Al_2O_3) was formed. The process described above can be summarized in the following reactions [**14**]. According to the data reported by Guzman-Castillo *et al.*, [**15**] and Rinaldial i and Schuchardt [**16**], the transition from boehmite to γ-Al_2O_3 takes place in the range of temperature 380-580°C.

$$2\ Al(OH)_{3(s)}\ (\text{bayerite}) \rightarrow 2AlO.OH_{(s)}\ (\text{boehmite}) + 2H_2O_{(g)} \quad \text{at } 300°C \quad (3)$$

$$2AlO.OH_{(s)}\ (\text{boehmite}) \rightarrow \gamma\text{-}Al_2O_3\ (s) + H_2O_{(g)} \quad \text{at } 500°C \quad (4)$$

$$2\ Al(OH)_{3(s)} \rightarrow \gamma\text{-}Al_2O_3\ (s) + 3H_2O_{(g)} \quad (5)$$

Figure 4 shows the XRD patterns of the various alumnias obtained at 500°C, compared with a commercial alumina. The equivalent crystallite sizes calculated by the scherrer formula [**17**], $D = k\lambda/(b \cos \theta)$, are shown in table 1. As can be seen in this figure 4 and in the crystallite sizes, the calcination of the gels at 500°C produced aluminum oxides of nano-crystalline structure, similar to that of commercial gamma alumina (surface area 220 $m^2 .g^{-1}$; crystalline size = 6nm).

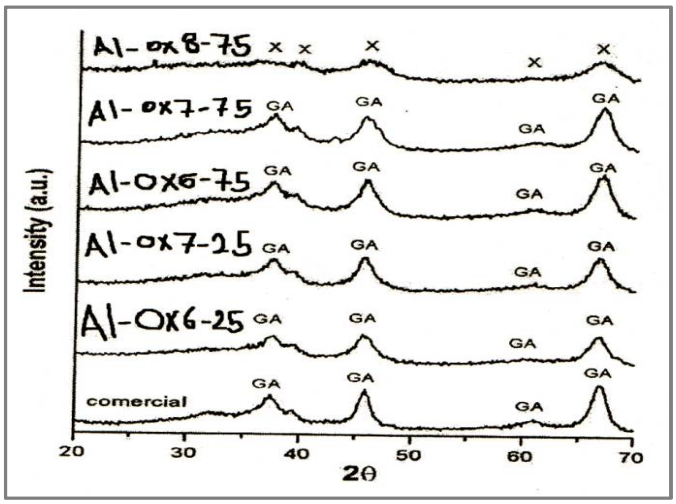

Figure 4. XRD patterns of different types of aluminas synthesized in this work and a commercial alumina (GA: γ- Al_2O_3; χ ; Chi-Al_2O_3).

The precipitation at pH 8 which is in the isoelectric point range of bayerite seemed not to favor the ordered growth of the bayerite g rains. Thus leading to the formation of a gel containing a minor phase of bayerite (figure 1); moreover, this pH favored the arrangement of highly crystalline gibbsite. The crystal growth of bayerite and gibbsite follows different pathways and as can be seen in the results of the present work, the crystal growth of the bayerite and gibbsite were strongly influenced by the precipitation pH.

Next, the XRD pattern of the aluminum oxide obtained by thermal treatment of G 8-75 at 500°C is attributed to the formation of poorly crystalline Chi-alumina. The Chi-alumina structure is based on a hexagonal close packed (hcp) structure of the oxygen atoms, where the aluminum cations occupy the octahedral site within the hexagonal oxygen layers. On the other hand, the γ-alumina structure has been described as a defect spinel structure , that can be represented by a face centered cubic (fcc) structure of oxygen atoms, with aluminum cations occupying the tetrahedrally and the octahedrally coordinated interstitial sites [**18**].

The results of textural analysis of the synthesized and commercial aluminum oxides are summarized in (Table 1). Analyzing the surface area of the samples in relation to their pH of precipitation, it is observed that the surface area of 278 $m^2 g^{-1}$ obtained at pH 6 (Al-Ox6-75) decreased to 195 $m^2 g^{-1}$ in the sample obtained at pH 8 (Al-Ox8-75), both samples having been aged at the same temperature of 75°C, a corresponding relation was found for samples obtained at 25°C. From these results it can be concluded that acidic precipitation (pH 6 and 7) increases the surface area of the material, in agreement with previous works [**19, 20**]. It is known 25°C that the surface area of aluminum depends on the extent of aggregation and dissolution of alumina gel grains during aging, which is strongly affected by the pH of precipitation .In this connection, it is observed that at acidic pH (pH = 6),

Table 1. Results of textural analysis of aluminum oxides carried out by the method of nitrogen adsorption–desorption (S_{BET}) and crystallite size (XRD)

Samples	Specific surface area ($m^2 g^{-1}$)	Average pore diameter (D_{avg}:nm)	Pore volume ($Cm^3 g^{-1}$)	Crystallite size (nm)
Al-Ox8-75	195	6.25	0.300	3.6
Al-Ox7-75	275	5.73	0.930	6.1
Al-Ox6-75	278	4.95	0.342	5.9
Al-Ox7-25	283	4.30	0.305	5.3
Al-Ox6-25	370	2.95	0.270	4.8

aggregation of grains of aluminum gel is probably favored, leading to the formation of oxides with smaller pores and high surface area, while at higher pH (pH 7-8) the dissolution of grains of alumina gel is favored, resulting in the formation of oxides with larger pores and lower surface area.

Panias and krestou [**21**] correlated the pH of precipitation of the gel to the crystallite size of the alumina formed. According to those authors, the crystallite sizes of the oxides increase with increasing pH, in both series of aluminas, aged at 25°C and 75°C see (Table 1). However, the crystallites obtained at pH 8 were the smallest among all the samples, owing to the amorphous structure of the Chi-alumina formed (figure 4). The increase in crystallite size caused at pH 7 suggests the enhancement of grain growth by dissolution–reprecipitation, during the aging treatment, favored at this precipitation pH, where the dissolution of boehmite and bayerite contained in the gel is favored, leading to aluminas of larger crystallites after thermal treatment at 500°C.

According to table 1, the decrease in surface area at pH 7 corresponds to the increasing crystallites size of the aluminas, relative to those aluminas synthesized at pH 6. The decrease in surface area at pH 8 cannot be understood in this way, since this sample has the lowest crystallite size. The surface area increased with decreasing crystallite size and reached a maximum when the crystallite size was 4.8 nm (370 $m^2 g^{-1}$ for Al-Ox 6-25).

Regarding the influence of aging temperature, it is observed that samples aged at 75°C had the largest pores diameter. This trend can be explained by the fact that during aging at high temperature, fewer grins of aluminum hydroxide are formed, allowing a more orderly growth of particles during this process and leading to the formation of oxides with larger pores and lower surface areas. Thus, it can be inferred that the dissolution of the gel of aluminum hydroxide formed is favored at 80°C. A contrary effect take place at room temperature 25°C, where many grains are formed, which hinder the orderly growth of particles, leading to the formation of oxides with small pores and thus a higher surface area table 1.

According to values in table 1, with increasing surface area, the average pore diameter (D_{Avg};nm) decreases in both series of aluminas those aged at 25°C and 75°C in the following order; from Al-Ox7-75 (crysttalite size = 6.0, D_{Avg} = 5.73 nm, surface area = 275 $m^2 g^{-1}$) to Al-Ox6 -75 (crysttalite size = 5.9, D_{Avg} = 4.95 nm, surface area = 278 m^2g^{-1}) and Al-Ox7 -25 (crysttalite size = 5.3, D_{Avg} = 4.30 nm, surface area = 283 $m^2 g^{-1}$) to Al-Ox6 -25 (crysttalite size = 4.8, D_{Avg} = 2.95 nm ,surface area = 370 $m^2 g^{-1}$). On the other hand, Al-Ox 8-75 has the smallest crystallite size (3.6 nm), which is smaller than its own average pore diameter (D_{Avg} = 6.25 nm), and thus a decrease in the surface area of this sample the lowest value recorded 195 $m^2 g^{-1}$ must come from the decrease in the number of pores, caused by the very small alumina crystals that probably block some surface pores.

Potdar *et al.*, [**22**] obtained γ-Al_2O_3 from boehmite synthesized from $Al(NO_3)_3$ and Na_2CO_3, at a slightly basic pH and aged at 70°C for 3h; the maximum surface area of that alumina was 258 $m^2.g^{-1}$. similarly Guzman-Castillo *et al.*,[**15**], prepared boehmite from solution of $Al2(SO_4)_3.18H_2O$, $AlCl_3$ and NH_4OH at pH 7-9 aged at 50, 140 and 180°C for 18 h, the maximum surface area of these aluminas was 248 $m^2 g^{-1}$. In these examples, the aging temperature and pH of precipitation are close to the conditions used in the present study.

One of the goals of the present study is to achieve the high surface area of these aluminas, especially those synthesized at room temperature, whose peak value was 370 $m^2 g^{-1}$ for sample Al-Ox6 -25. In other words, an alumina with high surface area was synthesized under mild conditions and relatively inexpensive reagent.

Adsorption isotherms of Cd and Pb on alumina are shown in (figure 5a, b). It can be seen that overall the isotherms are of type I, characteristic of microporous materials with formation of a mono-

layer of absorbate (respectively the ions Cd^{2+} , Pb^{2+}) on the surface of alumina, where each active center acts individually .

A mong the aluminas synthesized at room temperature, the average pore diameter of sample Al-Ox7-25 (D_{Avg} = 4.30 nm) is larger than that of Al- Ox 6-25 (D_{Avg} = 2.95 nm) ,which could explain the higher adsorption values of two cations on the first of these samples. The same reasoning can be applied to the series of aluminas obtained at 75°C, where the adsorption of each cations is higher on Al- Ox 7-75 (D_{Avg} = 5.73 nm) and Al-Ox8-75 (D_{Avg} = 6.25 nm) than on Al-Ox6-75 (D_{Avg} = 4.95 nm).

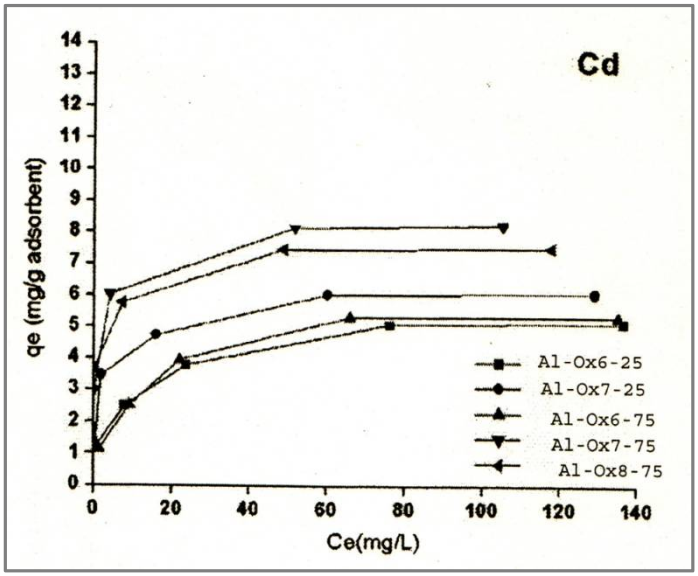

Figure 5a. Adsorption isotherms obtained on activated alumina under various conditions (a) cadmium.

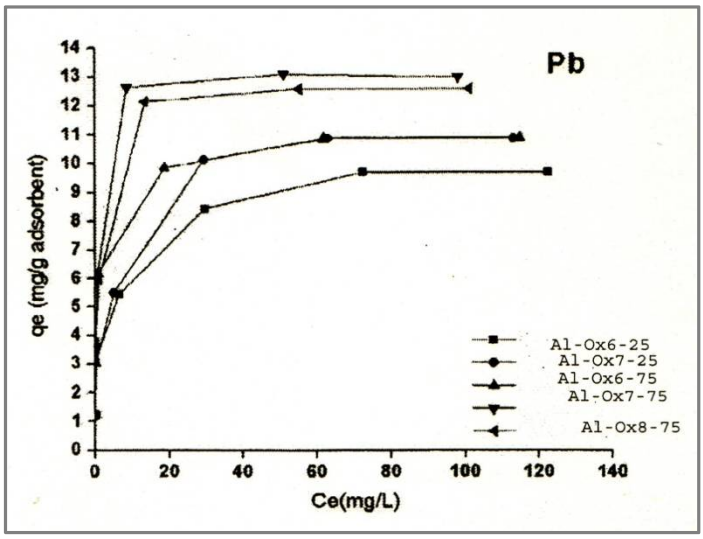

Figure (5b). Adsorption isotherms obtained on activated alumina under various conditions. (b) Lead.

These results suggest that the divalent cations are more readily adsorbed on surfaces with large pores. It can also be said that a precipitation pH of 7-8 and an aging temperature of 75°C, which led to the large hexagonal prism morphology, promoted the adsorption of these metals on the alumina surface, sample Al- Ox 7-75 showing the best overall performance, closely followed by Al-Ox8-75.

From the above discussion of adsorption assays, it can be seen that the Al-Ox7-75 was the best adsorbent for Cd^{2+} and Pb^{2+} ions. The profiles of the adsorption isotherms of cadmium and lead (figure 5) show that show that adsorption of these metals on Al-Ox 7- 75 has the following order of selectivity: Pb(II)> Cd (II), which follows the decreasing order of their atomic radii : Pb (1.75 Å) > Cd(1.54Å). Although the values of the ionic radii are less well –defined, their sequence must match that of atomic radii .It can be inferred that the size of the metallic species has an influence on the adsorption process. A larger ionic radius results in a weaker repulsion from the positively–charged alumina surface, favoring adsorption on larger pores.

Tables 2 and 3 show the correlation of the experimental adsorption results with the langmuir and freundlich models (Eqs. (1) and (2)) it is seen in these tables that the Langmuir model fits the data best, as shown by the higher correlation coefficient (R^2). In this model, the adsorption process takes place by the formation of a mono-layer of adsorbate (Cadmium, lead) on the surface of the alumina, where there is a finite number of homogeneous adsorption sites, energetically equivalent and with no interaction between them [23] (Table 4).

Table 2. Langmuir and Freundlich parameters for the adsorption of cadmium on the aluminas

Samples	Langmuir parameters (Cd) $q_{max}(mg.g^{-1})$	$b(L.g^{-1})$	R^2	Freundlich parameters (Cd) Kfn		R^2
Al-Ox6-25	5.35	0.14	0.99	1.62	4.06	0.98
Al-Ox7-25	6.10	0.43	0.99	2.25	4.10	0.92
Al-Ox6-75	5.68	0.14	0.99	2.80	1.12	0.95
Al-Ox7-75	8.26	1.80	0.99	5.95	4.15	0.98
Al-Ox8-75	7.51	1.33	0.99	5.54	3.63	0.85

Table 3. Langmuir and Freundlich parameters for the adsorption of lead on the aluminas

Samples	Langmuir parameters (Pb) $q_{max}(mg.g^{-1})$	$b(L.g^{-1})$	R^2	Freundlich parameters (Pb) Kfn		R^2
Al-Ox6-25	9.85	0.44	0.99	2.13	2.75	0.85
Al-Ox7-25	11.05	0.52	0.99	2.95	4.05	0.70
Al-Ox6-75	10.95	1.84	0.99	5.85	6.44	0.88
Al-Ox7-75	13.11	1.80	0.99	4.55	3.40	0.80
Al-Ox8-75	12.64	2.54	0.99	6.58	6.20	0.84

Table (4). Comparison of adsorption capacity (q_e) of various adsorbents for Pb (II), Cd (II) removal

Adsorbent	Weight of Adsorbent ($g\ L^{-1}$)	Cadmium $q_e(mg\ g^{-1})$	Lead $q_e(mg\ g^{-1})$	Reference
Activated alumina	8	8.26	13.12	Present work
Activated alumina	10	-	-	[24]
Activated bituminous carbons	4	-	-	[25]
Powder activated carbon	0.5	-	-	[26]
Activated alumina	7.5	6.3	-	[27]
Composite material:polystyrene Alumina/Carbon	10	-	10.64	[28]

APPLICATION

Today a wide variety of different synthesis strategies are proposed to obtain mesoporous alumina materials. The synthesis has to be chosen depending on the required properties such as ordered mesoporosity, high specific surface areas and pore volumes, crystallinity *etc*.

CONCLUSION

In this study it was possible by the method described to prepare various types of aluminum hydroxide from aluminum can which, when precipitation at pH 6-7 and then calcined at 500°C, led to the formation of γ-Al_2O_3. These aluminum hydroxides were synthesized from sodium aluminate (derived from aluminum scrap and sulfuric acid under several sets of conditions: pH 6-7 and 8 and aging temperatures of 25°C and 75°C. The samples prepared at lower pH had larger surface areas and smaller pores than their prepared at higher pH. Alumina aged at 75°C had larger pores, favoring the adsorption of voluminous ions such as lead. All adsorption isotherms of cadmium, lead were of type 1. The highest adsorption of cadmium was achieved on samples Al-OX7-75 (q_e = 8.26 mg g^{-1}). The highest values for lead adsorption were obtained with samples Al-OX7-75 (q_e = 13.11 mg g^{-1}) and Al-OX 8-75 (q_e = 12.64 mg g^{-1}). The alumin as synthesized in this work exhibited high adsorptive capacities showing a promising future for the utilization of alumina in the removal of Pb(II) and Cd(II) ions present in aqueous solution.

REFERENCES

1. T. K. Sheel, Preparation of aluminum Oxide from Industrial Waste Can Available in Bangladesh Environment: SEM and EDX Analysis, *Journal of Advanced Chemical Engineering*, **2016**, 6(2),
2. S. Chotisuwan, Mesoporous alumina prepared from waste aluminum cans and used as catalytic support for toluene oxidation .Material s Letters, **2012**, 70, 125-127.
3. Y. J. O. Asenciosa, M. R. Sun-koub, Synthesis of high surface area gamma-Al_2O_3 from aluminum scrap and its use for the adsorption of metals: Pb(II) ,Cd (II),and Zn (II), Optical Materials, **2012**, 34(9), 1553- 1557.
4. J. A. Fernando, D. D. L. Chung, Improving an alumina fiber filter membrane for hot gas filtration using an acid phosphate binder, *Journal of NaterialScience*, **2001**, 36, 5069-5085.
5. A. R. Keshavarz, M. Rezaei, F. Yaripour, Nanocrystalline gamma–alumina: A highly active catalyst for dimethyl ether synthesis, *Powder Technology*, **2010**, 199(2), 176-179.
6. Z. Zhang, T. J. Pinnavaia, Mesostructured forms of the transition phases η and χ- Al_2O_3, *Angewandte Chemie*, **2008**, 120(39), 7611-7614.
7. K. A. Matori, Phase transformations of α–alumina made from waste aluminum via a precipitation technique , International Journal of Molecular Science, **2012**, 13(12), 16812-16821.
8. S. A. Hosseini, A. Niaei, D. Salari, Production of γ- Al_2O_3 from kaolin, *Open Journal of Physical Chemistry*, **2011**, 1(2), 23-27.
9. B. An, Azeotropic distillation –assisted preparation of nanoscale gamma- alumina powder from waste oil shale ash, *Chemical Engineering Journal*, **2010**, 157(1), 67- 72.
10. J. O. Yvan, *Applied surface Science*, **2012**, 258, 10002- 10011.
11. S. A. Nada, *International Journal of Current Engineering and Technology*, **2017**, 7(1).
12. V. R. Leopoldo-constantio, K. Araki, D. Oliveira-Silva , *Quimica Nova* , **2002**, 25, 490- 498.
13. R. Rinaldi, Ph.D. Thesis, Brazil, **2005**. Available from: http://biq.iqm.unicamp.br/ arquivos/tests/ ficha71403.htm.
14. X. Carrier, E. Marceau, J. F. Lambert, M. Che, Transformation of γ-Al_2O_3 in aqueous suspension Alumina chemical weathering studied as a function of pH, *Journal of colloid and interface Science*, **2007**, 308, 429-437.
15. M. L. Guzman-Castillo, F. Hernandes-Beltran, J. J. Fripit, A. Rodriguez- Hernandez, R.Garcia de leon, J. Navarrete-Bolanos, A.Tobon-Cervantes, X. Bokhimi, Physicochemical properties of aluminas obtained from different aluminum salts, *Catalysis Today*, **2005**, 107-108, 874-878.
16. R. Rinald, U. Schchardt, On the paradox of transition metal- free alumina –catalyzed epoxidation with aqueous hydrogen peroxide, *Journal of catalysis*, **2005**, 236, 335-345.

17. H. Klug, L. Alexander, X-ray diffraction procedures for polycrystalline and Amorphous Materials, Wiley, New York, **1974**.
18. C. Meephoka, C. Chaisuk, P. Samparnpiboon, P. Praserthdam, Effect of phase composition between nano(and $-Al_2O_3$ on Pt/Al_2O_3 catalyst in CO oxidation, *Catalysis Communication*, **2008**, 9, 546-550.
19. K. Hellgardt, D. Chadwick, On the preparation of high surface area from nitrate solutions, *Industrial and Engineering Chemistry Research*, **1998**, 37, 405-411.
20. T. Ono, Y. Oguchi, O. Togari, Control of the pore structure of porous Alumina, In Preparation of Catalysts III, Elsevier Science Publishers B.V.Amsterdam, **1983**.
21. D. Panias, A. Krestou, Effect of synthesis parameters on precipitation of nanocrystalline boehmite from aluminate solutions, Powder Technology, **2007**, 175, 163-173.
22. H. S. Potdar, K. Jun, J. Woo, S. Kim, Y. Lee, Synthesis of nano –sized porous (-alumina powder via a precipitation/digestion route, *Applied Catalysis A: General*, **2007**, 321, 109-116.
23. A. Navarro, J. C. Lazo, N. Cuizano, M. R. SunKou, B. Llanos, Insight into removal of phenol from aqueous solution s by law cost adsorbent :clays versus algae, *Separation Science and Technology*, **2009**, 44, 2491-2509.
24. A. K. Bhattacharys, S. N.Mandal, S. K. Das, Adsorption of Zn(II) from aqueous solution by using different adsorbents, *Chemical Engineering Journal*, **2006**, 123, 43-51.
25. R. Leyva Ramos, L. A. Bernal Jacome, J. MendozaBarron, L. FuentesRubio, R. M. Guerrero Coronado, Adsorption of Zn(II) from an aqueous solution onto activated carbon, *Journal of Hazardous Materials*, **2002**, B90, 27-38.
26. Chungsying Lu, Huantsung Chiu, Adsorption of Zn (II) from water with purified carbon nanotube, *Chemical Engineering Science*, **2006**, 61, 1138-1145.
27. T. K. Naiya, A. K. Bhattacharya, S. K. Das, Adsorption of Cd(II) and Pb (II) from aqueous solution on activated alumina, *Journal of Colloid and Interface Science*, **2009**, 333,14-26.
28. R. A. K. Rao, S. Ikram, J. Ahmed, Adsorption of Pb (II) on a composite material prepared from polystyrene –alumina and activated carbon: Kinetic and thermodynamic studies, *Journal of the Iranian Chemical Society*, **2011**, 8, 931-943.